Plant Physiol. (1997) 115: 101–111

Regulation of Growth Anisotropy in Well-Watered and Water-Stressed Maize Roots[1]

I. Spatial Distribution of Longitudinal, Radial, and Tangential Expansion Rates

Benjamin M. Liang, Robert E. Sharp, and Tobias I. Baskin*

Department of Agronomy, Plant Science Unit (B.M.L., R.E.S.), and Division of Biological Sciences (T.I.B.), University of Missouri, Columbia, Missouri 65211

As a system to study the regulation of growth anisotropy, we studied thinning of the primary root of maize (*Zea mays* L.) occurring developmentally or induced by water stress. Seedlings were transplanted into vermiculite at a water potential of approximately −0.03 MPa (well-watered) or −1.6 MPa (water-stressed). The diameter of roots in both treatments decreased with time after transplanting; the water-stressed roots became substantially thinner than well-watered roots at steady state, showing that root thinning is a genuine response to water stress. To analyze the thinning responses we quantified cell numbers and the spatial profiles of longitudinal, radial, and tangential expansion rates separately for the cortex and stele. The results showed that there was no zone of isotropic expansion and the degree of anisotropy varied greatly with position and treatment. Thinning over time in well-watered roots was caused by rates of radial and tangential expansion being too low to maintain the shape of the root. In response to low water potential, cell number in both tissues was unchanged radially but increased tangentially, which shows that thinning was caused wholly by reduced cell expansion. Water stress substantially decreased rates of tangential and radial expansion in both the stele and cortex, but only in the apical 5 mm of the root; basal to this, rates were similar in well-watered and water-stressed roots. By contrast, as in previous studies, longitudinal expansion was identical between the treatments in the apical 3 mm but in water-stressed roots was inhibited at more basal locations. The results show that expansion in longitudinal and radial directions can be regulated independently.

The beautiful and adaptive forms of plants arise through the growth of component cells. Not only must plant cells control their overall rate of expansion but they must also control the rate of expansion in different directions. When expansion rates in different directions are not equal, growth is said to be anisotropic. Cells in a developing organ must expand anisotropically to build organs of specific shapes.

Anisotropic growth depends on anisotropic mechanical properties of the cell wall. For growth to be anisotropic, regions of the cell wall must deform (i.e. yield) at different rates in different directions. When considering the anisotropic deformation of any material in two dimensions, such as in the plane of a cell wall, one direction in the plane will have the maximum rate of deformation and the minimum rate must occur in the perpendicular direction (Green, 1980). Thus, growth anisotropy can be characterized by two terms: the direction in which the maximum growth rate occurs and the magnitude of growth anisotropy, which is defined by the ratio of maximum to minimum growth rate. For cell walls within growing organs, both the direction and magnitude of anisotropy must be specified for appropriate morphogenesis.

In growing cells the most prominent anisotropic wall elements are cellulose microfibrils. There is a large body of evidence from both algae and higher plants indicating that the direction of maximum growth rate is specified by the alignment of cellulose microfibrils (Hepler and Palevitz, 1974; Green, 1980; Taiz, 1984; Brown, 1985). This includes correlative studies in which the axis of maximum growth rate was found to be perpendicular to the direction of predominant microfibril alignment, and experimental studies in which cells induced to grow isotropically, either with inhibitors or hormones, deposited disorganized cellulose (Richmond, 1983; Weerdenburg and Seagull, 1988; Iwata and Hogetsu, 1989). Considerable evidence indicates that the alignment of cellulose microfibrils is controlled by the alignment of cortical microtubules (Gunning and Hardham, 1982; Cyr, 1994).

In contrast to the direction of maximum growth rate, we have no knowledge of what specifies the magnitude of growth anisotropy. There are several reasons for our ignorance. By far, most investigators have studied elongation only and have ignored expansion in diameter. Of the few studies in which expansion in diameter has been considered, growth anisotropy often remained constant, as, for example, in the giant internodes of *Nitella* sp. or *Chara* sp. (Green, 1958; Wasteneys and Williamson, 1993), which

[1] This work was supported by the University of Missouri Research Board (award no. RB-95038 to T.I.B.) and Food for the 21st Century Program (R.E.S.), by the Cooperative States Research Service, U.S. Department of Agriculture (under agreement no. 92-37304-7868 with T.I.B. and no. 95-37100-1601 with R.E.S. and W.G. Spollen), and by a grant from the U.S. Department of Energy (award no. 94ER20146 to T.I.B.), which does not constitute endorsement by that department of views expressed herein. This is a contribution from the Missouri Agricultural Experiment Station, journal series no. 12,647.

* Corresponding author; e-mail baskin@biosci.mbp.missouri.edu; fax 1–573–882–0123.

have been much used as model cells to relate the mechanical properties of the cell wall to expansion (Taiz, 1984). In other experiments in which growth anisotropy was changed (e.g. with inhibitors), only the control growth, which was highly anisotropic, was compared with the treated, which was fully isotropic. Thus, despite strong evidence that the direction of maximum growth rate is specified by the alignments of cortical microtubules and cellulose microfibrils, there is almost no evidence bearing on what controls the amount of growth in the minimum direction, i.e. the magnitude of growth anisotropy.

The objectives of this study were to quantify the magnitude of growth anisotropy in a system in which it varies, and then to determine whether that magnitude is controlled by the alignments of either cortical microtubules or cellulose microfibrils. For this analysis, we chose the maize (*Zea mays*) primary root. These roots are large and grow rapidly, much is known about their physiology, and their cell walls have a uniform texture, in contrast to the crossed-polylamellate texture of the cell walls of seedling stems of many dicots (Roland et al., 1975; Wardrop et al., 1979). Furthermore, we took advantage of a physiological treatment that changes the dimensions of the growth zone and the shape of the root. Sharp et al. (1988) reported that in maize primary roots growing at low water potential elongation is maintained preferentially toward the root apex, whereas in the same region the roots become thinner. These changes in growth are believed to be adaptive so that under limited water supply roots can concentrate their use of resources and can elongate at minimum cost to explore new soil volume for water (Sharp et al., 1990; Voetberg and Sharp, 1991).

To characterize growth anisotropy of a single cell such as a *Nitella* internode, it is sufficient to measure the length and diameter of the cell over time. However, for a multicellular organ such as a root, measurements of elemental elongation and diameter over time are not sufficient. While elongation at a given distance from the apex of the root must be the same in all tissues (otherwise the root would tear or cells would slip), expansion in the radial direction can have different rates at different radial positions. In other words, at a given distance from the apex, radial expansion rates in the stele and cortex need not be equal. Moreover, expansion that is perpendicular to elongation has two components, radial and tangential, and these do not have to be equal at a given location (Silk and Abou Haidar, 1986). In this paper we confine the use of the term "radial expansion" to expansion that occurs in the radial direction; to refer in general to expansion that is orthogonal to elongation (i.e. radial or tangential) we use the term "lateral expansion."

To separate radial and tangential terms and to determine whether different root tissues have different rates of lateral expansion and respond differentially to water stress, we analyzed the stele and cortex separately. In fact, many observations suggest that the stele and cortex play different roles in morphogenesis. For example, the stele has been suggested to exert a compressive force on the cortex and limit elongation, similar to the way in which the epidermis is considered to limit elongation in shoots (Burström, 1971). The cortex is sometimes the main site of increased lateral expansion when roots respond to hypoxia (de Wit, 1978) or are treated with exogenous growth hormones (Svennson, 1972), and the tissues contribute differentially to thickening in response to mechanical impedance (Wilson et al., 1977). The cortex, but not the stele, expands irregularly in roots growing into rock fissures (Zwieniecki and Newton, 1995). Finally, the cortex, the stele, or even the epidermis can be the primary tissue affected in *Arabidopsis thaliana* mutants with swollen roots (Benfey et al., 1993). In spite of such evidence, to our knowledge, lateral expansion rates have never been quantified separately for the tissues of any organ.

MATERIALS AND METHODS

Seeds of maize (*Zea mays* L. cv FR27 × FRMo17) were germinated for 34 h in moist vermiculite at 29°C and near-saturation humidity in the dark. Seedlings with radicles approximately 5 mm long were transplanted into Plexiglas boxes containing vermiculite at a water potential of either approximately −0.03 MPa (well-watered) or −1.61 ± 0.1 MPa (mean ± SD; water-stressed) and grown under the same conditions for up to 60 h (Sharp et al., 1988). Water potential of the vermiculite was determined by isopiestic thermocouple psychrometry in each experiment (Boyer and Knipling, 1965). Primary roots used for growth analysis were growing vertically within ± 10% of the mean elongation rate (approximately 3 mm h^{-1} for the well-watered treatment and 1 mm h^{-1} for the water-stressed treatment). To determine elongation rate the positions of the root apices were marked on the Plexiglas box several hours before and immediately prior to sampling. Illumination during transplanting, growth measurement, and harvesting was provided by a green safelight (Saab et al., 1992).

Root Diameter Measurements

The time dependence of root diameter change of well-watered and water-stressed roots was studied by harvesting roots at 6 and 12 h after transplanting and at 12-h intervals thereafter. Apical 15-mm segments were excised and viewed through a stereo-dissecting microscope, and the images were captured by a charge-coupled video camera (VI-470, Optronics Engineering, Goleta, CA) interfaced to an image analysis program (Image I, Universal Imaging, West Chester, PA). Root diameters were measured at equally spaced intervals along the root, with the distal end of the cap defined as zero (referred to here as the root apex).

Cell Numbers

To determine cell numbers in the stele and cortex, fresh cross-sections were cut by hand, and sections from three positions (2, 5, and 10 mm from the apex) were imaged at low magnification with a compound microscope and captured digitally as described above. To count cell layers, a diameter that did not cross metaxylem vessels was overlaid

with the image analysis program, and the number of cells that intersected the diameter was determined. These procedures were carried out four times on each section but at different angles, and the results for each tissue were averaged. To count the total number of cells in the inner stele, a circle was drawn with a radius going from the center of the root to the inner edge of the metaxylem cells, and cells within the circle were counted. To count total cortical cells, a diameter was drawn and all cortical cells on one side were counted, and the result was multiplied by 2 for the total.

Longitudinal Strain Rates

Longitudinal strain rates were measured at 24 (well-watered only) and 48 h (both treatments) after transplanting, essentially as described previously (Silk et al., 1984; Sharp et al., 1988). The face of the Plexiglas box was removed and the selected roots were dusted with graphite particles using a paint brush. The face was replaced and roots were allowed to recover for 1 h. Photographs were then taken at 15-min intervals for 1 h using a green safe-flash. Photographs were enlarged, and for each root, mark displacement was digitized on the set of five photographs to provide longitudinal velocity (mm h^{-1}) versus position, which was then interpolated to equally spaced intervals (0.5 mm) by spline fit, and differentiated with respect to position using Erickson's second-degree, five-point formula (Erickson, 1976) to give the profile of longitudinal strain rate (h^{-1}). Only those roots with a maximum velocity that recovered to at least 90% of the premarking elongation rate were used for the strain rate analysis.

Lateral Strain Rates

Lateral strain rate measurements were made at the same times after transplanting and in roots selected with the same criteria as for measurements of longitudinal strain rate. Fresh cross-sections were cut by hand at 0.5-mm intervals in a glass Petri dish on filter paper moistened with deionized water (for well-watered roots) or with an aqueous solution of PEG 8000 (365 mg mL^{-1}) having a water potential of −1.6 MPa. Preliminary trials showed that this solution did not cause sections of water-stressed roots to shrink or swell detectably. After cross-sections were cut, they were imaged through the dissecting microscope and captured as described above. Diameters of the whole root and of the stele were measured at four different angles and averaged. For water-stressed roots, this procedure was repeated three times for each root to reduce measurement error. The diameter of the cortex was taken as the difference between the diameters of the whole root and the stele and thus includes the epidermis. Lateral strain rates ($R[z]$ h^{-1}) were then calculated as:

$$R(z) = \left(\frac{1}{D[z]}\right) \times V(z) \times \left(\frac{\delta D}{\delta z}\right) \quad (1)$$

where z denotes the longitudinal distance from the root apex, $D(z)$ is the diameter, $V(z)$ is the longitudinal velocity, and $\delta D/\delta z$ is the spatial gradient of the diameter (Silk and Abou Haidar, 1986). The term $\delta D/\delta z$ was calculated for data points in the apical 4 mm with Erickson's second-degree, five-point differential formula and for points beyond 4 mm with the seven-point differential formula (Erickson, 1976). We opted for this method because we could not find a function that fitted the root diameter versus position data without systematic deviations.

Lateral strain rate has two specific components, tangential and radial, named after their directional vectors. These terms are equal when the elemental rate of expansion is the same for all radii and at all radial positions; otherwise, expansion rates in radial and tangential directions will differ. Because the root maintains its circular shape in the cross-section, all radii are essentially equivalent. But because the root is divided into different tissues, expansion at different radial distances from the center may differ. For the stele, radial landmarks (e.g. metaxylem cells) are not uniform among sections; therefore radial and tangential rates were assumed to be equal, and a single lateral expansion rate was calculated by substituting the diameter of the stele for D in Equation 1. For the cortex the tangential term was calculated by substituting the total root diameter for D and thus strictly applies to the epidermis; the radial term was found by substituting the cortex diameter for D.

To assess the variability of lateral strain rates, experiments were repeated on different days. For each experiment, diameter versus position data were averaged and used to calculate the spatial gradient of diameter and the lateral strain rate. These parameters from the different experiments were then averaged and are presented with the associated SEs. The results were not noticeably different when lateral strain rates were computed separately for each root and then averaged or when the diameters of all roots were averaged and a single lateral strain rate was computed. Lateral strain rates could not be calculated strictly independently for each root because the longitudinal velocity data were obtained in separate experiments.

The spatial profile of diameter of well-watered roots was changing at 24 h; therefore, we evaluated time-dependent changes in lateral strain rates. These were calculated as:

$$\epsilon(z) = \left(\frac{1}{D[z]}\right) \times \left(\frac{\delta D[z]}{\delta t}\right) \quad (2)$$

where $\epsilon(z)$ is the relative time-dependent variation, and $\delta D(z)/\delta t$ is the change in diameter over time. The temporal gradient of diameter was obtained by measuring diameters in sections as described above at 19, 24, and 29 h after transplanting and applying Erickson's three-point differential formula to data for diameter versus time at each measured position (1-mm intervals) to obtain the slope at the middle point. At each position, Equation 2 was used to calculate temporal diameter changes of the whole root, cortex, and stele, and these corrections were added to strain rates calculated from Equation 1 for tangential and radial strain in the cortex and lateral strain in the stele, respectively.

RESULTS

Time Course of Root Diameter Changes

It was noticed before that seedling roots of maize and other species thin when grown at a low water potential (Taylor and Ratliff, 1969; Sharp et al., 1988); however, at least in maize, well-watered roots also get progressively thinner with time from germination (Sharp et al., 1988; Fraser et al., 1990). In these studies diameters were measured at no more than one or two times, so we do not know the time course of diameter change for either the well-watered or water-stressed treatments, nor whether steady-state values of diameter eventually occur. Therefore, water deficit could cause roots to thin more than they would during normal development or instead could cause them to thin faster but not to a greater extent. To distinguish between these alternatives, we measured the diameters of well-watered and water-stressed roots as a function of time.

In both treatments roots thinned at all positions between 1 and 10 mm from the apex (Fig. 1, only selected positions shown). By 24 h after transplanting the elongation rate was at steady state in the water-stressed roots and in the well-watered roots was nearly at steady state, increasing only slightly over the next 36 h (Fig. 1, inset). By contrast, root diameter required longer times to reach steady state, taking 48 h in well-watered roots and at least 60 h in the water-stressed roots. Except at 1 mm from the apex, water-stressed roots became substantially thinner than the steady-state value of well-watered roots, showing that low water potential caused roots to thin to a greater extent than did development. It should be noted that the apical centimeter of the water-stressed roots maintains a high relative water content as a result of osmotic adjustment (Sharp et al., 1990), and therefore the reduced diameter was not caused by lack of tissue hydration.

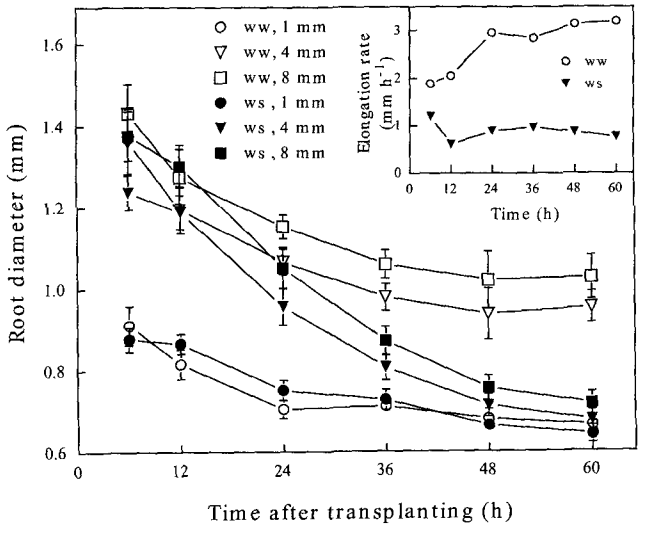

Figure 1. Time course of diameter changes at 1, 4, and 8 mm from the apex of maize primary roots following transplanting into vermiculite at a water potential of either −0.03 MPa (well-watered, ww) or −1.6 MPa (water-stressed, ws). Data are means ± SD (n = 14–16, combined from three replicate experiments). The inset shows elongation rates for the same roots, with data plotted at the end of each measurement interval.

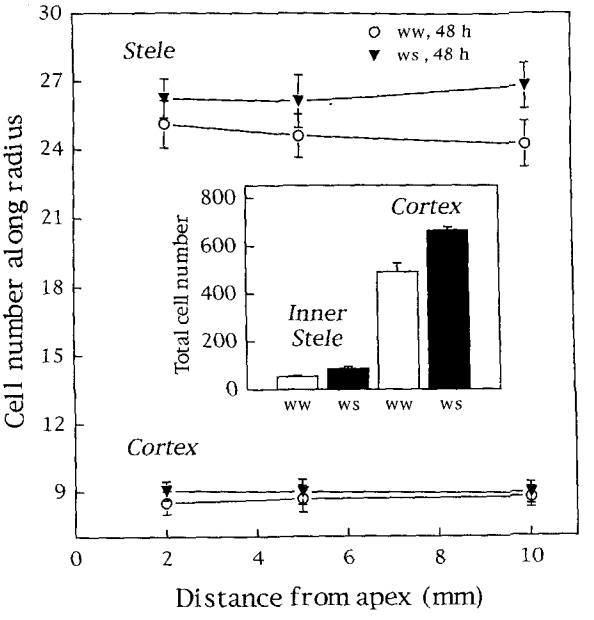

Figure 2. Cell layers and total cell numbers as a function of distance from the apex for well-watered (ww) and water-stressed (ws) roots 48 h after transplanting. The inset shows total cell number measured at 10 mm from the apex for the cortex and inner stele (all cells lying within a circle reaching to the inner edge of metaxylem cells). Data are means ± SD (n = 16–29 for cell layers, n = 7–9 for total cell number from three experiments).

As a result of this time course, we analyzed the developmental thinning of well-watered roots by comparing roots at 24 and 48 h after transplanting, and we analyzed the effects of water stress by comparing roots 48 h after transplanting, when lateral expansion of well-watered roots had reached steady state and that of water-stressed roots was nearly at steady state. We chose 24 and 48 h so that the treatments would be comparable with those of earlier studies (Sharp et al., 1988, 1990; Spollen and Sharp, 1991; Wu et al., 1994, 1996).

Cell Number Changes

To determine whether the thinning response to low water potential involved changes in cell division, we counted cells in fresh cross-sections at defined positions of well-watered and water-stressed roots 48 h after transplanting. In each treatment the number of radial cell layers at 10 mm from the apex was indistinguishable from that at 2 mm in both the stele and cortex (Fig. 2), showing that periclinal cell divisions were rare or absent beyond 2 mm. When the treatments were compared, the number of cell layers was nearly equal, with only slight (if any) increases in the water-stressed roots. Also, the number of metaxylem vessels was slightly greater in the water-stressed roots (6.7 ± 0.73 versus 6.4 ± 0.81 for well-watered; mean ± SD, measured at 10 mm from the apex). A similar slight increase of radial layers in water-stressed roots of the same age was

reported by Fraser et al. (1990). When cells were counted along a circumference (not shown) or total cells were counted for each tissue, the water-stressed roots were found to have substantially more cells than the well-watered roots (35% more for the cortex, 62% more for the stele; Fig. 2, inset). Evidently, low water potential stimulated cell division primarily in the anticlinal (longitudinal radial) plane, increasing cell numbers in both tissues. The increase in cell number in the water-stressed roots shows that the root thinning response was determined wholly by restricting cell expansion.

Spatial Distribution of Longitudinal Strain Rate

The spatial distributions of longitudinal displacement velocity and longitudinal strain rate for the 24-h well-watered treatment and for the 48-h water-stressed treatment (Fig. 3) were similar to those previously obtained (Sharp et al., 1988; Saab et al., 1992). Elongation rate was unaffected by low water potential in the apical 3 mm but was progressively inhibited at more basal locations, reaching 0 at just over 7 mm. In the well-watered roots, strain rate increased to a peak at 4.5 mm and then decreased to 0 beyond 11 mm. The velocity and strain rate profiles of the well-watered roots at 48 h were very similar to those at 24 h, except that the zone of elongation was slightly longer (Fig. 3), accounting for the slightly greater root elongation rate (Fig. 1, inset).

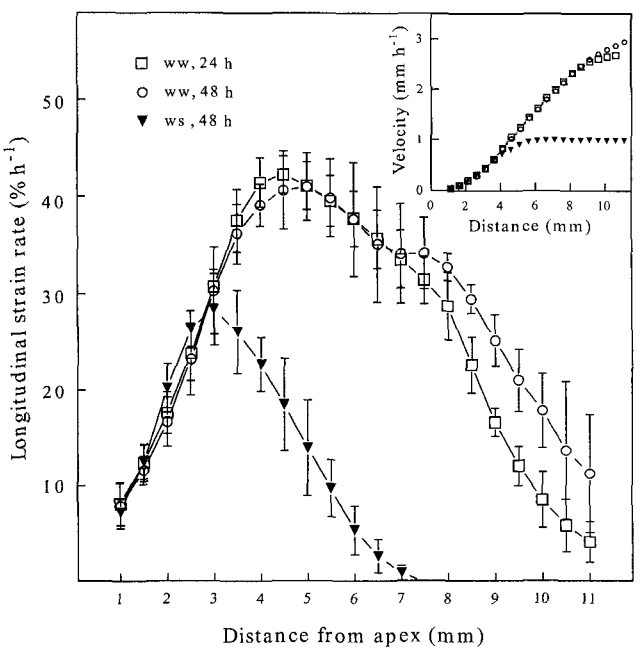

Figure 3. Longitudinal strain rates as a function of distance from the apex of well-watered (ww) and water-stressed (ws) roots. Data are means ± SD (n = 6–7 from three to seven experiments) for well-watered roots at 24 and 48 h and for water-stressed roots at 48 h. The inset shows longitudinal velocity profiles for the same roots, with error bars omitted for clarity.

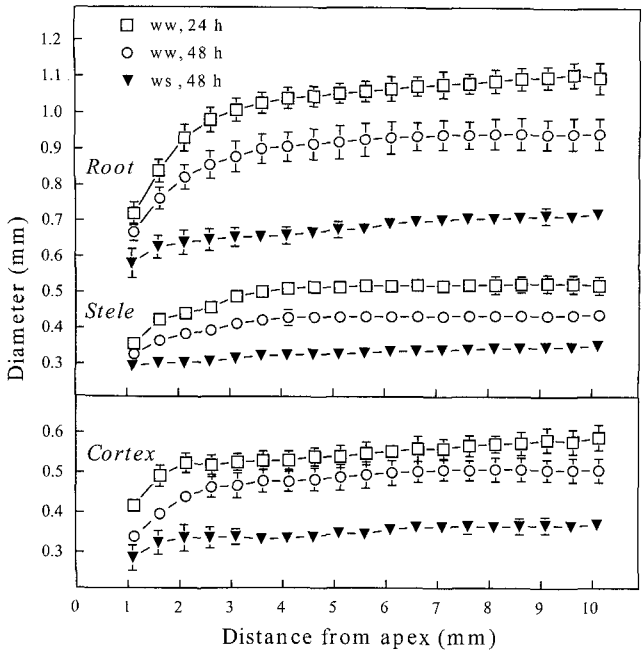

Figure 4. Diameter profiles of the apical 10 mm of well-watered (ww) and water-stressed (ws) roots. Whole-root and stele diameters were measured directly from fresh sections, and that of the cortex was obtained as the difference between the whole root and the stele. Data are means ± SD for well-watered roots at 24 h (n = 12, from two experiments) and at 48 h (n = 11, from three experiments) and for water-stressed roots at 48 h (n = 11, from three experiments).

Profiles of Diameter for Root, Stele, and Cortex

We measured the profiles of root and tissue diameters in fresh cross-sections to avoid changes in size from fixation, embedding, or sectioning. Overall root diameter increased relatively steeply with position in the apical region of the root and then increased much more gradually (Fig. 4). The transition from steep to gradual increase occurred at a more apical position in water-stressed than in well-watered roots. In water-stressed and well-watered roots at 24 h, diameter increased gradually to the end of the sampled region, whereas for the well-watered roots at 48 h, diameter became constant by approximately 9 mm from the apex. The changes in overall root diameter, both developmental and due to water stress, involved significant changes in the diameter of both the stele and cortex throughout the sampled region (Fig. 4). The stele had more shallow increases in diameter in the apical region compared with the cortex. Beyond 5 mm from the apex for well-watered roots the diameter of the cortex increased gradually but that of the stele remained constant, whereas for water-stressed roots the diameter of both tissues increased gradually.

To calculate lateral strain rates, one needs the spatial gradient in diameter ($\delta D/\delta z$, Eq. 1). This gradient had a similar shape for all tissues, having a maximum value at the most apical point and declining to nearly 0 by 5 mm from the apex (Fig. 5). In the apical region the gradient was steeper for well-watered roots than for water-stressed roots, and for the well-watered roots was steeper at 24 h than at 48 h (Fig. 5). In both treatments the gradient was

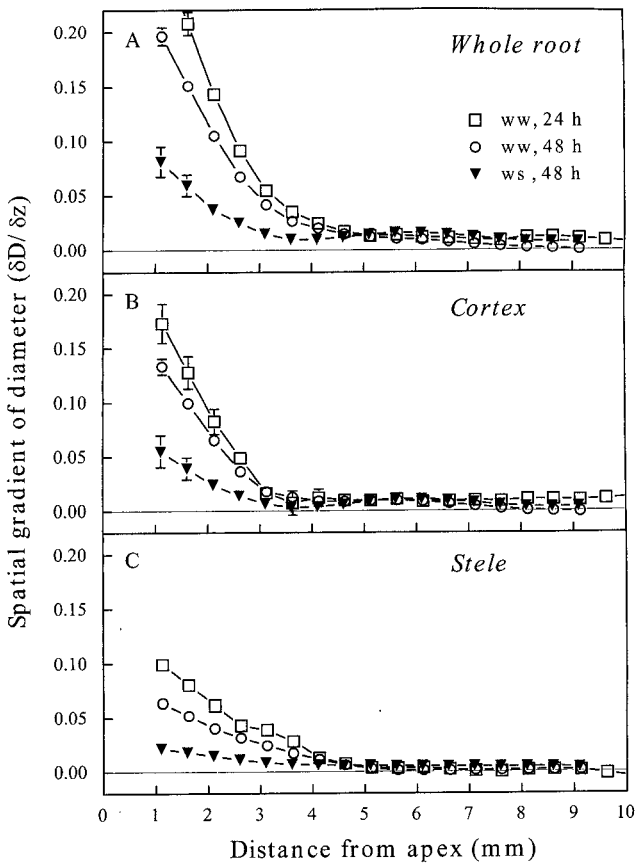

Figure 5. Spatial gradient of diameter of the whole root (A), the cortex (B), and the stele (C) for well-watered (ww) and water-stressed (ws) roots. To assess variability, average root diameters were calculated from each of three (48-h well-watered and water-stressed) or two experiments (24-h well-watered), and a spatial gradient was calculated for each. These were then averaged and the SES calculated, which are plotted when larger than the symbol. Total sample sizes were 11 roots for the 24-h well-watered treatment and 12 roots for each of the other treatments.

steeper for the cortex than the stele. At positions basal of 5 mm the gradient was low in all cases; the gradient actually reached 0 for only the stele of the 24-h well-watered treatment and the stele and cortex of the 48-h well-watered treatment at the most basal positions sampled (Fig. 5).

Spatial Distribution of Lateral Strain Rates

Lateral strain rate was calculated from longitudinal velocity (Fig. 3, inset), diameter (Fig. 4), and the gradient in diameter (Fig. 5), according to Equation 1. In the cortex of well-watered roots at 48 h after transplanting, radial and tangential strain rates had a similar pattern, having a bimodal distribution with maxima at approximately 2 and 6 mm from the apex (Fig. 6, A and B). Comparable levels of lateral expansion occurred in the apical and basal regions of the growth zone because of balanced, opposing differences in the spatial gradient in diameter and in longitudinal velocity: for the apical maximum, diameter increased steeply with position but longitudinal velocity was low, whereas for the basal maximum, diameter increased gradually with position but longitudinal velocity was high.

In contrast to the cortex, lateral expansion in the stele had a single peak located between 3 and 4 mm from the apex, where radial strain in the cortex was low. In the apical 5 mm of both the stele and cortex, radial and tangential strain rates were 2- to 3-fold higher in the well-watered than in the water-stressed roots. In contrast, beyond 5 mm from the apex, the rates of radial and tangential strain were virtually the same in the two treatments. These patterns of lateral expansion show that thinning of water-stressed roots is caused by a major restriction of lateral strain rates in the apical 5 mm of both the stele and cortex.

To compare lateral strain rates between 24 and 48 h in the well-watered roots, it was necessary to correct the lateral strain rates at 24 h for time-dependent changes in diameter. Figure 7 shows lateral strain rates for the 24-h well-watered treatment with and without the correction term. Because the roots thinned over time, the correction term is negative.

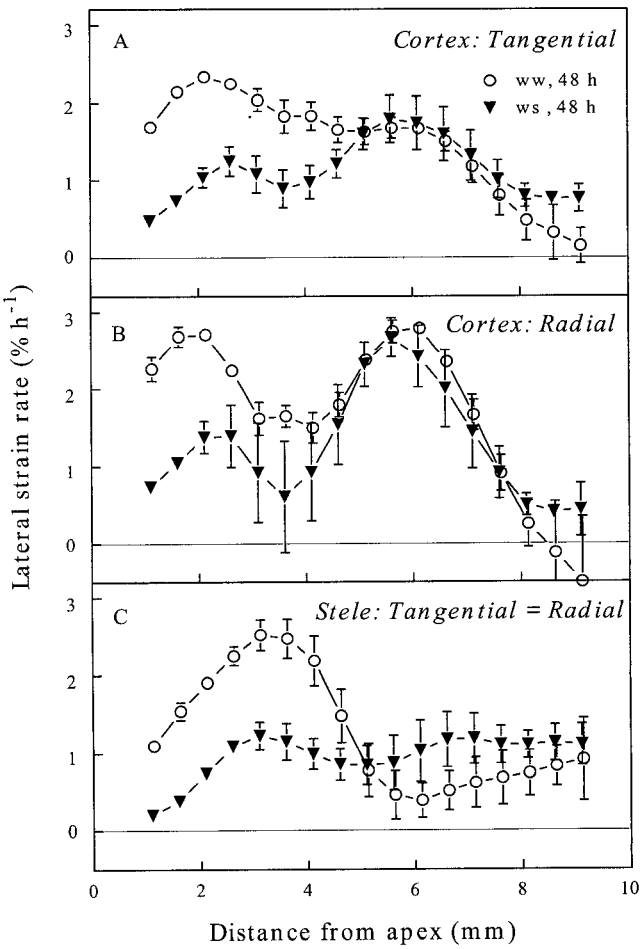

Figure 6. Lateral strain rates as a function of distance from the apex of well-watered (ww) and water-stressed (ws) roots at 48 h after transplanting. A, Tangential strain rate for the cortex; B, radial strain rate for the cortex; and C, lateral (radial = tangential) strain rate for the stele. Rates were calculated separately for each of the experiments listed in the legend for Figure 5 and averaged. Error bars show the SE when larger than the symbol.

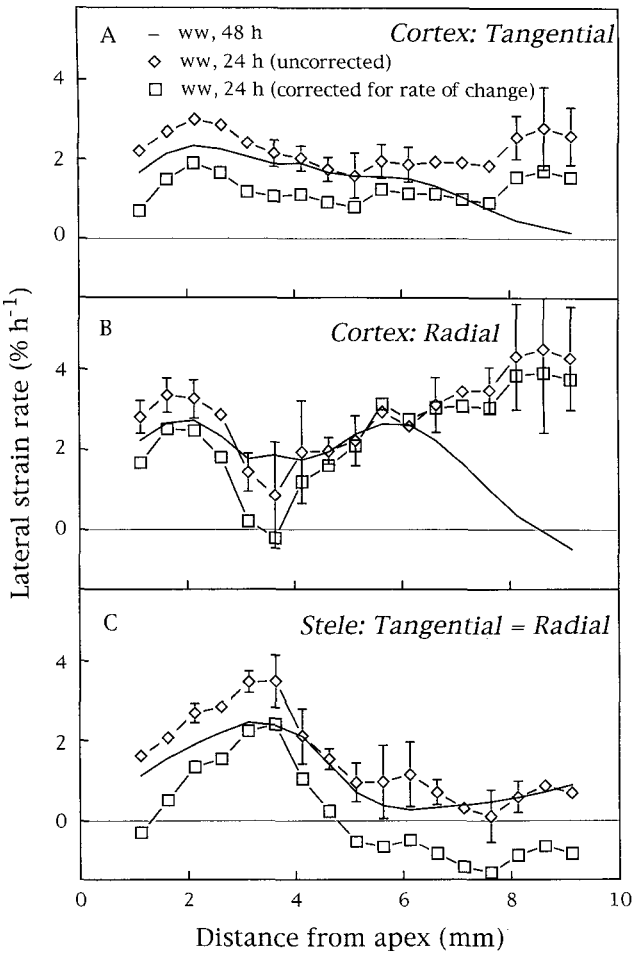

Figure 7. Comparison of lateral strain rates between well-watered (ww) roots 24 and 48 h after transplanting. A, Tangential strain rate for the cortex; B, radial strain rate for the cortex; and C, lateral (tangential = radial) strain rate for the stele. Rates at 24 h were calculated separately for two experiments as described in the legend for Figure 5 and averaged. Results are plotted before (±SE) and after correction for time-dependent thinning, calculated using the procedure described in "Materials and Methods" and applied to eight roots for each of three sampled times from two experiments. The results for 48-h well-watered roots are shown as a solid line and are redrawn from Figure 6.

The magnitude of the correction term is on the order of 1% per hour, which amounts to a significant correction. For tangential strain in the cortex and the stele (Fig. 7, A and C) the magnitude of the time-dependent term was largely independent of position, whereas for radial strain in the cortex (Fig. 7B), thinning over time was restricted mostly to the apical 5 mm of the root. For the stele, the corrected strain rates were negative beyond 5 mm from the apex, implying that at 24 h the basal portion of the stele was shrinking.

In Figure 7 the lateral strain rates for well-watered roots at 48 h are shown as a solid line. Comparing them with the corrected data at 24 h shows that, in general, the shapes of the curves at the two times were similar and that in the cortex, as at 48 h, appreciable lateral expansion occurred throughout most of the growth zone. The magnitude of lateral strain rate was generally lower at 24 than at 48 h, with the notable exception of radial strain rates in the cortex beyond 6 mm from the apex, which increased to high values in contrast to the steady decline seen at 48 h (Fig. 7B). This difference in radial strain rates in the basal part of the cortex is reflected by the diameter of the cortex (Fig. 4), which beyond 6 mm from the apex expanded steadily at 24 h but remained constant at 48 h. This high rate of cortical radial expansion beyond 6 mm from the apex might have compressed the stele, causing the shrinkage seen in that tissue in the same region.

Growth Anisotropy

With the spatial profiles of both longitudinal and lateral strain thus calculated, we could assess the magnitude of growth anisotropy and compare it between well-watered and water-stressed treatments. The magnitude of anisotropy is expressed conveniently as the ratio of longitudinal to lateral strain; when this ratio equals 1, expansion is isotropic, and when the ratio is greater than 1, the major direction of expansion is longitudinal.

In Figure 8 we plotted the logarithm of this ratio and omitted points near the end of the sampled region, where the small values of longitudinal and lateral strain drive the ratio to 0 or infinity. In each treatment the spatial profile of anisotropy was similar in the cortex and stele, but the patterns were very different between the treatments (Fig. 8). For well-watered roots (only the 48-h data are shown for clarity), the magnitude of anisotropy increased with increasing distance from the apex, from approximately 5 at 1 mm from the apex to values of nearly 100 between 6 and 8 mm from the apex. In contrast, for the water-stressed roots, the magnitude of anisotropy was well above 10 for the apical 4 mm and then decreased steeply at more basal locations.

DISCUSSION

Despite widespread acceptance that morphogenesis, i.e. the production of organic form, is an important problem of plant physiology, there have been surprisingly few studies in which rates of lateral expansion have been characterized. To our knowledge, we are the first to quantify lateral strain rates in different tissues. Several features of lateral expansion have emerged that illuminate root morphogenesis.

Lateral Expansion in the Basal Region of the Growth Zone

Our results show that in well-watered maize primary roots radial and tangential strain continues at substantial rates throughout most of the region where longitudinal strain occurs. Moreover, in water-stressed roots lateral strain rates in the basal region of the growth zone are comparable to well-watered roots, in contrast to the large difference between treatments in longitudinal strain rates in the same region. For primary roots of a different cultivar of maize grown under nearly the same conditions as used here, Sharp et al. (1988) calculated a combined radial and

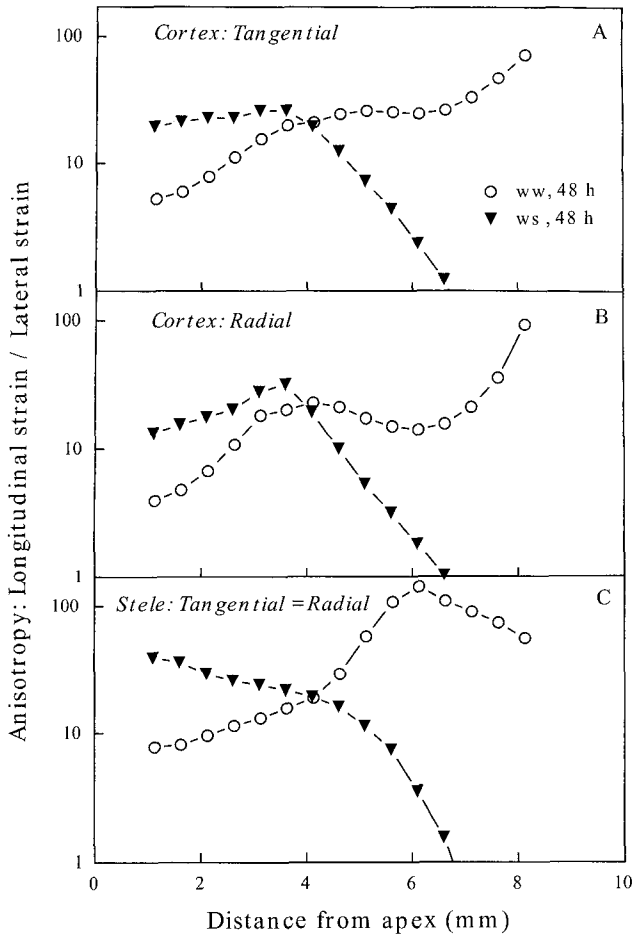

Figure 8. Growth anisotropy as a function of distance from the apex of well-watered (ww) and water-stressed (ww) roots 48 h after transplanting. Longitudinal strain rates were divided by lateral strain rates: A, Longitudinal divided by tangential strain rate of the cortex; B, longitudinal divided by radial strain rate of the cortex; and C, longitudinal divided by lateral strain rate of the stele. Note that the *y* axes are plotted on a logarithmic scale, and values near the basal end of the growth zone that were either extremely large or less than 1 were omitted.

tangential strain rate by obtaining a tangential strain rate according to Equation 1 and multiplying it by 2 to include the radial contribution, assumed to be equal. For the water-stress treatment, they reported a bimodal distribution for radial plus tangential strain, which is very similar to twice that shown here for tangential strain (Fig. 6A). For well-watered roots, they used a 20-h treatment but did not account for the time-dependent change in diameter; therefore, their distribution should be compared with twice the uncorrected tangential data for 24 h (Fig. 7A). When compared in this way, their well-watered distribution is similar to ours, except that lateral expansion rates in the basal region of the growth zone were even greater than those shown here.

The maintenance of significant lateral expansion rates throughout the growth zone found here and by Sharp et al. (1988) conflicts with the way in which lateral expansion is often thought to vary in roots. Lateral expansion rate has been equated with the spatial profile of diameter, so that regions of the root that are highly curved are the only regions assumed to have high rates of lateral expansion (e.g. García-Sánchez et al., 1991). However, the spatial gradient in diameter does not contain any information about how long it takes for an element to move from one point on the gradient to the next; instead, that information is contained in the spatial profile of longitudinal velocity.

In the maize root apical positions are steeply curved (Fig. 4) but have relatively low longitudinal velocity (Fig. 3, inset), whereas more basal positions have only slight increases in the spatial gradient of diameter (Fig. 5) but have high velocity; as a result, both regions have significant lateral expansion. For example, in the cortex of 24-h well-watered roots, the radial expansion rate at 8 mm from the apex was actually greater than the peak near the meristem (Fig. 7B). In the basal regions of the root growth zone, the large longitudinal velocity means that even small increases in root or tissue diameter with position require significant lateral expansion rates.

Maintenance of lateral expansion rates in the basal part of the growth zone does not agree with results of Barlow et al. (1991) in a study of excised tomato roots, which to our knowledge is the only report of lateral strain rates for roots of a species other than maize. These authors reported that radial expansion occurred only in a limited region in the apical part of the root growth zone. Although this difference may reflect the differences in plant material, to obtain the spatial gradient of diameter needed for the calculation, Barlow et al. (1991) fitted a sigmoid function to data for cortical cell width versus position. This approach has two difficulties: (a) cell width data are very noisy, and (b) curve fitting imposes the character of the function on the data. Both the scatter in the cell width data and the smooth function used could have obscured the small changes in diameter that result from significant lateral expansion rates in the basal part of the growth zone. To determine whether lateral strain rates are often maintained throughout the root growth zone, they must be quantified under a variety of circumstances and in several species. As shown here, doing so requires attention to time-dependent changes in diameter, as well as to small changes in diameter that occur where longitudinal velocity is high.

The profiles of growth anisotropy shown in Figure 8 for well-watered maize roots are completely different from that inferred by Baluška et al. (1996, and refs. therein). These authors contended that between the zones of cell division and elongation only, at approximately 2 to 3 mm from the tip, there is a "zone of more-or-less isotropic cell growth in which the cells both elongate and increase in width at similar rates" (Baluška et al., 1996). The lack of polarity of cell expansion claimed for this region framed their interpretations of observations of cytoskeletal and other constituents of the root (Baluška et al., 1996). However, all of their statements about rates of cellular expansion, longitudinal as well as lateral, come from analysis of cell shapes in median longitudinal sections. Plots of cell shape versus position contain no information about the rate of cellular expansion; for this, one must know how fast

a cell moves from one position to the next, i.e. its longitudinal displacement velocity. This is true for radial expansion as explained above and also for elongation (Gray and Scholes, 1951; Hejnowicz and Brodzki, 1960; Green, 1976; Silk, 1992).

As shown in Figure 8, the zone between 2 and 3 mm from the apex had rates of longitudinal expansion about 10 times greater than lateral rates. At the position where cortical cells are isodiametric, the ratio of longitudinal to radial relative expansion rate shown in Figure 8B will equal the ratio of longitudinal to radial expansion rate per cell, invalidating the assumption of isotropic expansion for cells in this region of the root.

Developmental Changes in Diameter

In well-watered roots the lateral strain rates calculated at 24 h were notably lower than those at 48 h throughout most of the growth zone. This may seem paradoxical insofar as at 24 h the roots were thicker (Fig. 4). Apparently, after transplanting, the roots do not have high enough lateral expansion rates to maintain their shape, and thus they thin over time (Fig. 1). This was particularly notable for the stele, in which the low lateral expansion rate accounted for a considerable part of the total root thinning. Eventually, steady state is reached as the lateral strain rates become large enough to maintain the shape of the root over time.

One might speculate that a large diameter enhances the establishment of the seedling radicle, perhaps through provision of a solid structure, which then does not need to be maintained as the root grows out. Developmental changes in root diameter probably occur often among plants, because diameter is an important parameter of root architecture, but we have been unable to find published data quantifying root diameter versus time. As shown here, the morphological response of a root to its environment cannot be fully studied without also studying the morphological changes programmed by development.

Differences between the Stele and Cortex

Both the stele and cortex contributed to root thinning over time in well-watered roots and in response to low water potential. However, we found that the spatial distribution of lateral strain rate in the cortex differed notably from that of the stele. The cortex maintained tangential and radial expansion rates to near the end of the sampled region, whereas in the stele rates of lateral expansion were at low values beyond 5 mm from the apex (Fig. 7). Additionally, between 3 and 4 mm from the apex in the cortex there was a trough in radial strain rate, but in the stele there was a peak (Fig. 7, B and C). We cannot explain the opposite behavior of the tissues in this region, but it underscores the importance of resolving the lateral expansion of multicellular organs into component tissues.

Thinning of Water-Stressed Roots

Our data confirm and extend the findings of Sharp et al. (1988) and of Fraser et al. (1990); the diameter of water-stressed roots becomes substantially less than the steady-state diameter of well-watered roots, which shows that thinning of water-stressed roots is a genuine response to low water potential. It was suprising that thinner roots under water stress contained more cells, because of stimulated cell division specifically in the anticlinal (longitudinal-radial) plane. In contrast, water stress is known generally to inhibit transverse divisions, i.e. the so-called proliferative divisions of the meristem (González-Bernáldez et al., 1968; Meyer and Boyer, 1972). A recent study of rates of transverse cell division in maize primary roots, grown under similar conditions as used here, found that water stress indeed decreased the rate of transverse cell proliferation in most of the meristem (Sacks et al., 1997).

The adaptive significance, if any, of the larger number of cells under water stress is not known. Cell number was increased mainly in the circumference of the root. These additional cells will increase the total cellular surface area and provide more apoplastic pathways between cells for water and solute movement into and out of the root. Either the increased cellular surface area or the enlarged apoplastic pathway could aid water absorption and compensate for the surface area lost because of the thinning of the root.

Lateral strain rates of the water-stressed roots did not reach 0 by 9 mm from the apex (Fig. 6) even though longitudinal strain rates had reached 0 by 7.5 mm (Fig. 3). Thus, the data indicate that lateral expansion continues in the water-stressed roots in the absence of longitudinal expansion. However, because the gradient in velocity was small in the basal region, our method for measuring longitudinal strain may not be sensitive enough to have detected low values comparable to the lateral strain rates between 7.5 and 9 mm from the apex (approximately 0.5% h^{-1}). Additionally, the diameter of the water-stressed roots had not quite reached steady state by 48 h (Fig. 1), and thus their lateral strain rates were overestimated slightly.

Lateral expansion rates responded dramatically to water stress in the apical 5 mm of the root, where they were lowered by 50% or more. In contrast, at positions basal of 5 mm there was little difference between treatments (Fig. 6). This pattern is the opposite of what happened to longitudinal strain rates, which were the same in well-watered and water-stressed roots in the apical region but not in the basal region (Fig. 3). It is striking that at 6 to 8 mm from the apex, where radial and tangential strain rates in the cortex for the two treatments were virtually superimposable, longitudinal strain rates for water-stressed roots declined to 0 but for the well-watered roots were high and nearly steady. These data show that plants can vary their rates of longitudinal and lateral expansion independently.

Previous studies in this system found that turgor pressure is approximately constant in the first 10 mm of the root and approximately 0.4 MPa higher in well-watered than in water-stressed roots (Spollen and Sharp, 1991). Because turgor is lower but elongation rates are equal, these authors hypothesized that the apical region of the water-stressed roots has an increased cell wall extensibility. Consistent with this hypothesis, the apical 5 mm of water-stressed roots, compared with that of well-watered roots,

was shown to have greater acid-induced longitudinal wall extension (Wu et al., 1996) and higher activities of xyloglucan endotransglycosylase and expansin (Wu et al., 1994, 1996), which are probably both involved in wall loosening. We found, for the same region, that radial and tangential expansion rates are greatly decreased by water stress, indicating that whatever bonds are being broken or remade to increase extensibility in the longitudinal direction do not likewise increase lateral extensibility. By the same token, at 5 to 10 mm from the apex, longitudinal extensibilities are very different between the treatments (Wu et al., 1996), yet lateral expansion rates are very similar. Here too, longitudinal expansion rates are apparently controlled independently of radial and tangential rates. Independent control of longitudinal and lateral expansion must now be addressed by models that attempt to relate cell wall structure and metabolic activity to cell wall expansion.

CONCLUSIONS

Results from this study characterize the three-dimensional expansion that is needed to produce a plant organ with a specific shape. The results show that expansion in the maize primary root is highly anisotropic and, moreover, that the magnitude of anisotropy varies as a function of tissue, position, and treatment. The rate of lateral expansion is greater in the cortex than the stele at some positions, whereas at other positions that of the stele is greater, which argues against a dominant role in morphogenesis for either tissue. Thinning due to water stress is caused by restriction of lateral expansion in both the stele and cortex but only in the apical 5 mm of the root; basal to this, lateral expansion is nearly identical to that of well-watered roots. This pattern of response is the opposite of how longitudinal expansion responds, which is identical between the treatments apically and differs basally, showing that expansion rates in length and in width are regulated independently. Whether the magnitude of anisotropic expansion and the thinning response to water stress are controlled by the alignments of cortical microtubules or cellulose microfibrils is the subject of the next paper in this series.

ACKNOWLEDGMENTS

We acknowledge the contribution made in the initial stages of the work by Dr. Nirit Bernstein (Volcani Center, Israel). We thank Prof. Wendy Silk (University of California, Davis) for helpful discussions about the mathematical treatment of the nonsteady state and Dr. Gerrit Beemster for insightful comments concerning the manuscript.

Received March 27, 1997; accepted June 8, 1997.

LITERATURE CITED

Baluška F, Volkmann D, Barlow PW (1996) Specialized zones of development in roots. View from the cellular level. Plant Physiol **112:** 3–4

Barlow PW, Brain P, Parker JS (1991) Cellular growth in roots of a gibberellin-deficient mutant of tomato (*Lycopersicon esculentum* Mill.) and its wild-type. J Exp Bot **42:** 339–351

Benfey PN, Linstead PJ, Roberts K, Schiefelbein JW, Hauser M-T, Aeschbacher RA (1993) Root development in Arabidopsis: four mutants with dramatically altered root morphogenesis. Development **119:** 57–70

Boyer JS, Knipling EB (1965) Isopiestic technique for measuring leaf water potentials with a thermocouple psychrometer. Proc Natl Acad Sci USA **54:** 1044–1051

Brown RM Jr (1985) Cellulose microfibril assembly and orientation: recent developments. J Cell Sci Suppl **2:** 13–32

Burström HG (1971) Tissue tensions during cell elongation in wheat roots and a comparison with contractile roots. Physiol Plant **25:** 509–513

Cyr RJ (1994) Microtubules in plant morphogenesis: role of the cortical array. Annu Rev Cell Biol **10:** 153–180

de Wit MCJ (1978) Morphology and function of roots and shoot growth of crop plants under oxygen deficiency. *In* DD Hook, RMM Crawford, eds, Plant Life in Anaerobic Environments. Ann Arbor Science, Ann Arbor, MI, pp 333–350

Erickson R (1976) Modeling of plant growth. Annu Rev Plant Physiol **27:** 407–434

Fraser TE, Silk WK, Rost TL (1990) Effects of low water potential on cortical cell length in growing regions of maize roots. Plant Physiol **93:** 648–651

García-Sánchez C, Casero PJ, Lloret PG, Navascués J (1991) Morphological changes and transversal growth kinetics along the apical meristem in the pericycle cell types of the onion adventitious root. Protoplasma **160:** 108–114

González-Bernáldez F, López-Sáez JF, García-Ferrero G (1968) Effect of osmotic pressure on root growth, cell cycle and cell elongation. Protoplasma **65:** 255–262

Gray LH, Scholes ME (1951) The effect of ionizing radiations on the broad bean root. Part VIII: Growth rate studies and histological analyses. Br J Radiol **24:** 82–92, 176–180, 228–236, 285–291, 348–352

Green PB (1958) Structural characteristics of developing *Nitella* internodal cell walls. J Biophys Biochem Cytol **4(5):** 505–515

Green PB (1976) Growth and cell pattern formation on an axis: critique of concepts, terminology, and mode of study. Bot Gaz **137:** 187–202

Green PB (1980) Organogenesis—a biophysical view. Annu Rev Plant Physiol **31:** 51–82

Gunning BES, Hardham AR (1982) Microtubules. Annu Rev Plant Physiol **33:** 651–698

Hejnowicz Z, Brodzki P (1960) The growth of root cells as the function of time and their position in the root. Acta Soc Bot Pol **29:** 625–644

Hepler PK, Palevitz BA (1974) Microtubules and microfibrils. Annu Rev Plant Physiol **25:** 309–362

Iwata K, Hogetsu T (1989) Orientation of wall microfibrils in *Avena* coleoptiles and mesocotyls and in *Pisum* epicotyls. Plant Cell Physiol **30:** 749–757

Meyer RF, Boyer JS (1972) Sensitivity of cell division and cell elongation to low water potentials in soybean hypocotyls. Planta **108:** 77–87

Richmond PA (1983) Patterns of cellulose microfibril deposition and rearrangement in *Nitella*: in vivo analysis by a birefringence index. J Appl Polymer Sci **37:** 107–122

Roland JC, Vian B, Reis D (1975) Observations with cytochemistry and ultramicrotomy on the fine structure of the expanding walls in actively elongating plant cells. J Cell Sci **19:** 239–259

Saab IN, Sharp RE, Pritchard J (1992) Effect of inhibition of abscisic acid accumulation on the spatial distribution of elongation in the primary root and mesocotyl of maize at low water potentials. Plant Physiol **99:** 26–33

Sacks MM, Silk WK, Burman P (1997) Effect of water stress on cortical cell division rates within the apical meristem of primary roots of maize. Plant Physiol **114:** 519–527

Sharp RE, Hsiao TC, Silk WK (1990) Growth of the maize primary root at low water potentials. II. Role of growth and deposition of

hexose and potassium in osmotic adjustment. Plant Physiol **93:** 1337–1346

Sharp RE, Silk WK, Hsiao TC (1988) Growth of the maize primary root at low water potentials. I. Spatial distribution of expansive growth. Plant Physiol **87:** 50–57

Silk WK (1992) Steady form from changing cells. Int J Plant Sci Suppl **153:** S49–S58

Silk WK, Abou Haidar S (1986) Growth of the stem of *Pharbitis nil*: analysis of longitudinal and radial components. Physiol Veg **24:** 109–116

Silk WK, Walker RC, Labavitch J (1984) Uronide deposition rates in the primary root of *Zea mays*. Plant Physiol **74:** 721–726

Spollen WG, Sharp RE (1991) Spatial distribution of turgor and root growth at low water potentials. Plant Physiol **96:** 438–443

Svensson SB (1972) A comparative study of the changes in root growth, induced by coumarin, auxin, ethylene, kinetin and gibberellic acid. Physiol Plant **26:** 115–135

Taiz L (1984) Plant cell expansion and regulation of cell wall mechanical properties. Annu Rev Plant Physiol **35:** 585–657

Taylor HM, Ratliff LF (1969) Root elongation rates of cotton and peanuts as a function of soil strength and soil water content. Soil Sci **108:** 113–119

Voetberg GS, Sharp RE (1991) Growth of the maize primary root at low water potentials. III. Role of increased proline deposition in osmotic adjustment. Plant Physiol. **96:** 1125–1130

Wardrop AB, Wolters-Arts M, Sassen MMA (1979) Changes in microfibril orientation in the walls of elongating plant cells. Acta Bot Neerl **28:** 313–333

Wasteneys GO, Williamson RE (1993) Cortical microtubule organization and internodal cell maturation in *Chara corallina*. Bot Acta **106:** 136–142

Weerdenburg C, Seagull RW (1988) The effects of taxol and colchicine on microtubule and microfibril arrays in elongating plant cells in culture. Can J Bot **66:** 1707–1716

Wilson AJ, Robards AW, Goss MJ (1977) Effects of mechanical impedance on root growth in barley, *Hordeum vulgare* L. II. Effects on cell development in seminal roots. J Exp Bot **28:** 1216–1227

Wu Y, Sharp RE, Durachko DM, Cosgrove DJ (1996) Growth maintenance of the maize primary root at low water potentials involves increases in cell-wall extension properties, expansin activity, and wall susceptibility to expansins. Plant Physiol **111:** 765–772

Wu Y, Spollen WG, Sharp RE, Hetherington PR, Fry SC (1994) Root growth maintenance at low water potentials. Increased activity of xyloglucan endotransglycosylase and its possible regulation by abscisic acid. Plant Physiol **106:** 607–615

Zwieniecki MA, Newton M (1995) Roots growing in rock fissures: their morphological adaptation. Plant Soil **172:** 181–187